A time-averaged model for gas/solids flow in a one-dimensional vertical channel

Sofiane Benyahia
National Energy Technology Laboratory, Morgantown, WV 26505

Abstract

In this study, we are interested in deriving time-smoothed governing and constitutive equations for gas/solids flow in moderately-dense systems where particle-particle collision is the main energy dissipation mechanism. Apart from Reynolds stresses, constitutive relations for the solids phase and gas/solids friction coefficient are highly non-linear and Taylor series expansion of these expressions required many terms that did not always converge due to large-scale oscillations in all flow variables computed using the transient model. The Euler transformation was used in some cases so that the Taylor series expansions converge. This yields a large number of correlations, especially between solids volume fraction and granular temperature, which makes this steady-state model less likely to be used as an "engineering model" as in the case single-phase turbulence modeling. The computed steady-state solution was same as the time-averaged solution obtained using transient model.

Introduction

Gas/solids flows are commonly encountered in industry, such as fossil fuel, nuclear and pharmaceutical technologies. For a couple of decades, mathematical models based on granular kinetic theory have been used mainly in academia and rarely in industry due to the long computational time required to conduct gas/solids flow simulation in large-scale devices. For example, it takes several hours to compute a grid-independent gas/solids flow in a simple one-dimensional (1-D) vertical channel (Benyahia et al. 2007). Therefore, this study attempts the derivation of a time-smoothed gas/solids flow model that can potentially be used as a reduced order model (ROM) by industry. Such a practice is common in single-phase flow turbulence where the equations are time- or Reynolds-averaged and "engineering models", such as k-epsilon model, are used to close the time-independent correlation that arise from the only non-linear convection term.

Most studies in the literature that investigated time-averaging of multiphase flow equations were conducted for dilute (solids volume fraction less than 0.1 %) flows where particle-particle interactions may be ignored, such as the work of Elghobashi and Abou-Arab (1983) who derived a fluid-phase k-epsilon turbulence model. Dasgupta et al. (1994) derived a k-epsilon model for gas/solids flows assuming small particles so that no distinction is made between gas and solids velocity components. They applied their model to dense flows by using simplified forms of solids pressure and viscosity that are independent of granular temperature. To our knowledge only one study of time-averaged gas/solids flow equations using the granular kinetic theory was rigorously derived by Hrenya and Sinclair (1997). They recognized the importance of non-linear terms, such as the dissipation of granular energy. However, they used only a first order approximation of the Taylor series expansion of the non-linear dissipation term. Furthermore, the time-averaging of the production of granular energy was not conducted in previous studies, as the importance of this term was only recently demonstrated by Benyahia et al. (2007) who indicated that core-annulus flow regime cannot be predicted without proper averaging of this term. The assumption of small-

scale fluctuations lead previous researchers to approximate non-linear terms with 0^{th} and 1^{st} order terms in Taylor series as well as to neglect 3^{rd} order correlations in convective terms, which will be demonstrated to be inaccurate in this study.
We have used in our study a transient gas/solids flow model based on granular kinetic theory that gave us the ability to validate the Taylor expansion of non-linear terms as well as to neglect some correlations arising from averaging of convective terms. It was necessary to include many terms in these Taylor series expansions because of large oscillations in the gas/solids flow variables that were computed using the transient model. Furthermore, the Taylor series expansion of some constitutive relations, such as granular energy dissipation term, diverged and the Euler transformation was used to ensure the convergence of these series. Thus, the major advantage of this study over previous studies is the ability to generate computational data using a transient model based on the open-source MFIX code (www.mfix.org), which allowed for detailed analysis of most non-linear terms in the time-averaged gas/solids flow model.

Simulation conditions

This study is conducted for a gas/solids flow in a 1-D channel of 10-cm width using air at ambient conditions and glass beads of 120 microns diameter and 2.4 g/cm^3 density. A particle-particle restitution coefficient of 0.99 is used in this study. Both the vertical and horizontal velocity components are solved for. However, we used periodic boundary conditions with only one computational cell along the vertical or y-component; thus, all derivatives with respect to y will vanish except for the gas pressure. Traditionally, the MFIX solver used a fixed gas pressure-drop along the flow-wise, or y, direction, but it is now possible to specify a fixed gas mass flow rate and the gas pressure drop will be adjusted using Newton's algorithm to achieve the specified gas flow rate within a specified tolerance. Constant domain-averaged gas velocity and solids volume fraction of 5.5 m/s and 0.03, respectively, are used in this study. At the walls, simple boundary conditions (BC) are used: free slip for the solids velocity and zero flux for granular temperature. The value of restitution coefficient close to unity and a zero flux BC for granular temperature are chosen to diminish the amplitude of large-scale oscillations that increase with increasing energy dissipation due to particle-particle and particle-wall collisions as demonstrated by Benyahia et al. (2007). All computational results are expressed in CGS (cm, grams, and seconds) unless otherwise specified. Numerical and other physical parameters used in this study are the same as those used by Benyahia et al. (2007).

Derivation of time-averaged governing equations for gas-solids flow

The mass and momentum balances used in this study were derived by Gidaspow (1994) using the volume averaging technique and have been widely used in the chemical engineering literature to model multiphase flows. In this study, we only focus our attention on time-averaging the solids governing equations because the large-scale oscillations that occur in this relatively dense flow are due to the formation of clusters that can be captured with sufficient accuracy using a transient flow model based on granular kinetic theory (Agrawal et al. 2001, Benyahia et al., 2007).

The instantaneous solids continuity equation for a pseudo 1-D flow and constant solids density:

$$\frac{\partial}{\partial t}\left(\varepsilon_s\right) + \frac{\partial}{\partial x}\left(\varepsilon_s u_s\right) = 0$$

The time-averaged solids continuity is,

$$\frac{\partial}{\partial x}\left(\overline{\varepsilon_s u_s}\right) = 0$$

The Reynolds decomposition of the instantaneous variables into time-averaged and fluctuating parts:

$$\overline{\varepsilon_s u_s} = \overline{\left(\overline{\varepsilon_s} + \varepsilon_s'\right)\left(\overline{u_s} + u_s'\right)} = \overline{\varepsilon_s}\ \overline{u_s} + \overline{\varepsilon_s' u_s'}$$

Thus, the continuity equation becomes:

$$\frac{\partial}{\partial x}\left(\overline{\varepsilon_s}\ \overline{u_s}\right) + \frac{\partial}{\partial x}\left(\overline{\varepsilon_s' u_s'}\right) = 0 \qquad [1]$$

The solids horizontal instantaneous momentum equation:

$$\rho_s\left[\frac{\partial}{\partial t}\left(\varepsilon_s u_s\right) + \frac{\partial}{\partial x}\left(\varepsilon_s u_s u_s\right)\right] = -\ \varepsilon_s \frac{\partial P_g}{\partial x} + \frac{\partial \tau_{sxx}}{\partial x} - I_{gsx}$$

Where $\frac{\partial \tau_{sxx}}{\partial x} = -\frac{\partial P_s}{\partial x} + \frac{\partial}{\partial x}\left[\left(\eta\mu_b + 4/3\mu_s\right)\frac{\partial u_s}{\partial x}\right]$ and $I_{gsx} = \beta\left(u_s - u_g\right)$

Let's assume that the gas phase doesn't influence the horizontal motion of the solids; then the time-averaged horizontal momentum equation becomes:

$$\rho_s \frac{\partial}{\partial x}\left[\left(\overline{\varepsilon}_s \overline{u}_s \overline{u}_s\right) + \overline{\varepsilon_s' u_s' u_s'} + \overline{\varepsilon}_s \overline{u_s' u_s'} + 2\overline{u}_s \overline{\varepsilon_s' u_s'}\right] = -\frac{\partial \overline{P_s}}{\partial x} + \frac{\partial}{\partial x}\left[\overline{\left(\eta\mu_b + 4/3\mu_s\right)\frac{\partial u_s}{\partial x}}\right] \qquad [2]$$

The instantaneous solids vertical (main flow direction) momentum equation:

$$\rho_s\left[\frac{\partial}{\partial t}\left(\varepsilon_s v_s\right) + \frac{\partial}{\partial x}\left(\varepsilon_s u_s v_s\right)\right] = -\ \varepsilon_s \frac{\partial P_g}{\partial y} + \frac{\partial \tau_{sxy}}{\partial x} - I_{gsy} - \rho_s \varepsilon_s g$$

Where $\frac{\partial \tau_{sxy}}{\partial x} = \frac{\partial}{\partial x}\left(\mu_s \frac{\partial v_s}{\partial x}\right)$ and $I_{gsy} = \beta\left(v_s - v_g\right)$

The time-averaged vertical solids momentum equation becomes:

$$\rho_s \frac{\partial}{\partial x}\left[\left(\overline{\varepsilon}_s \overline{u}_s \overline{v}_s\right) + \overline{\varepsilon_s' u_s' v_s'} + \overline{\varepsilon}_s \overline{u_s' v_s'} + \overline{u}_s \overline{\varepsilon_s' v_s'} + \overline{v}_s \overline{\varepsilon_s' u_s'}\right] = -\ \overline{\varepsilon_s \frac{\partial P_g}{\partial y}} + \frac{\partial}{\partial x}\left(\overline{\mu_s \frac{\partial v_s}{\partial x}}\right) - \overline{I}_{gsy} - \rho_s \overline{\varepsilon}_s g \qquad [3]$$

The instantaneous granular temperature equation:

$$\frac{3}{2}\rho_s\left[\frac{\partial \varepsilon_s \Theta_s}{\partial t} + \frac{\partial \varepsilon_s u_s \Theta_s}{\partial x}\right] = \frac{\partial}{\partial x}\left(\kappa_s \frac{\partial \Theta_s}{\partial x}\right) + \tau_{sxx}\frac{\partial u_s}{\partial x} + \tau_{sxy}\frac{\partial v_s}{\partial x} - \rho_s J_s$$

For this particular case-study, we can neglect $\tau_{sxx}\frac{\partial u_s}{\partial x}$ because of the term $\tau_{sxy}\frac{\partial v_s}{\partial x}$. Thus, the time-averaged granular temperature equation becomes:

$$\frac{3}{2}\rho_s \frac{\partial}{\partial x}\left[\overline{\varepsilon}_s \overline{u}_s \overline{\Theta}_s + \overline{\varepsilon_s' u_s' \Theta_s'} + \overline{\varepsilon}_s \overline{u_s' \Theta_s'} + \overline{u}_s \overline{\varepsilon_s' \Theta_s'} + \overline{\Theta}_s \overline{\varepsilon_s' u_s'}\right] = \frac{\partial}{\partial x}\left(\overline{\kappa_s \frac{\partial \Theta_s}{\partial x}}\right) + \overline{\mu_s \frac{\partial v_s}{\partial x}\frac{\partial v_s}{\partial x}} - \rho_s \overline{J}_s \qquad [4]$$

Apart from the gravitational force in the vertical momentum equation [3], all terms in the time-averaged gas/solids governing equations are non-linear. The convective terms yield correlations of volume fraction, the two velocity components and granular temperature. There are 9 correlations from the convective terms in this pseudo 1-D model (we sometimes use the term pseudo 1-D because 1-D models usually solve only one component of velocity as the other component is neglected for fully-developed flows).

Transient simulations

We first conduct transient simulations based on the instantaneous governing equations to analyze the transient behavior of the gas/solids flow. This type of simulations was previously conducted and details are explained by Benyahia et al. (2007). We show here transient results of flow variables at three horizontal locations in the 1-D channel.

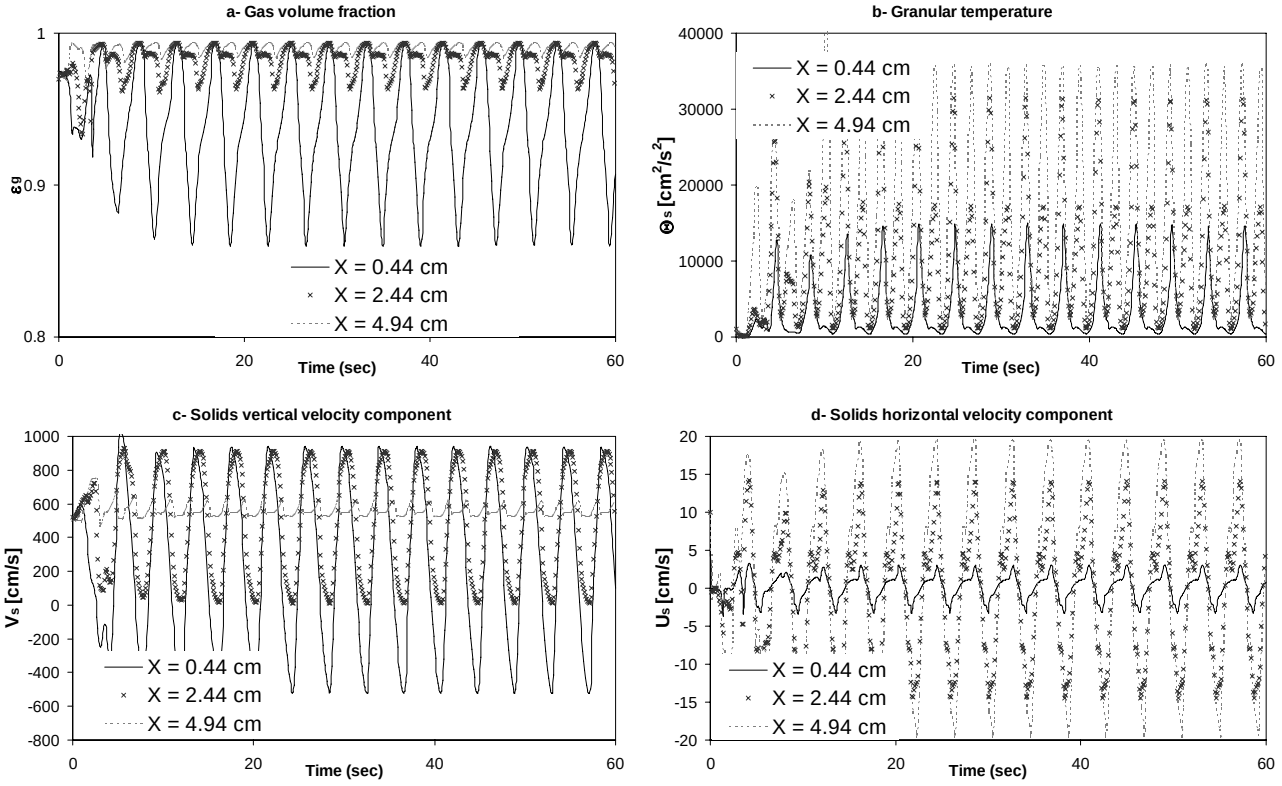

Figure 1 Transient profile of flow variables at three different locations (near the wall and at ¼ and ½ the channel width) in the 10-cm wide channel.

Figure 1 shows the large-scale fluctuations in the 1-D channel computed at three different locations (x=0.44 cm or near the wall, x=2.44 cm or half the distance between the center of the channel and the wall, and x=4.94 cm or the middle of the channel). An animation of the solids (or gas) volume fraction in the channel shows dense clusters of solids forming, alternatively, at one sidewall or the other in the 1-D channel similar to those computed by Benyahia et al. (2007). The motion of the large-scale clusters creates the oscillatory behavior observed in figure 1. After the initial transient behavior of few seconds, periodic oscillations are observed in all the flow variables at all locations. This is due to transient clusters that form periodically at one sidewall of the channel or the other. The largest deviations from the mean in the gas

volume fraction and solids vertical velocity are observed near the walls of the channel where clusters form and flow downward. On the other hand, the largest amplitude of oscillation in the granular temperature is observed at the center of the channel where the flow is relatively dilute. Also the solids horizontal velocity is small near the walls because the horizontal component of solids and gas velocities are set to zero at walls, and largest deviations from the mean (zero) are observed at the center of the channel where the flow is dilute. An important fact to notice in Figure 1 is that the amplitude of the oscillations is large, so that these are not the same type of fluctuations as in single-phase flow turbulence. In fact, it is clear from Figure 1 that there is only one frequency of oscillations as the small-scale fluctuations usually observed in single-phase turbulence are not computed in this 1-D channel flow.

Constitutive relations

The constitutive relations are based on the kinetic theory for granular flow (KTGF) model derived by Gidaspow (1994). This model is similar to other "dry" granular models, such as that of Lun et al. (1984), where the dissipation of granular energy is only due to inelastic collisions. Also this model ignores corrections to the solids viscosity and conductivity for very dilute flows, which is a reasonable assumption since this study involves a moderately dense flow. These simplifications make it easier to analyze the non-linear constitutive relations derived from kinetic theory because of their dependence on solids volume fraction and granular temperature only.
The constitutive relations derived from kinetic theory are the following:
Solids granular viscosity μ_s and conductivity κ_s :

$$\mu_s = \frac{\mu}{\eta g_0}\left[1+1.6\eta g_0 \varepsilon_s\right]^2 + 0.6\mu_b \qquad [5]$$

where dilute viscosity is: $\mu = \frac{5\sqrt{\pi}}{96}\rho_s d_p \sqrt{\Theta_s}$ and bulk viscosity: $\mu_b = \frac{8}{3\sqrt{\pi}}\rho_s d_p \varepsilon_s^2 g_0 \eta \sqrt{\Theta_s}$ and the radial distribution function: $g_0 = \frac{1}{\varepsilon_g} + 1.5\frac{\varepsilon_s}{\varepsilon_g^2} + 0.5\frac{\varepsilon_s^2}{\varepsilon_g^3}$ and $\eta = \frac{1+e}{2}$, $\varepsilon_g = 1-\varepsilon_s$.

$$\kappa_s = \frac{\kappa}{\eta g_0}\left[1+2.4\eta g_0 \varepsilon_s\right]^2 + 1.5\mu_b \qquad [6]$$

Where dilute granular conductivity is: $\kappa = \frac{75\sqrt{\pi}}{96}\rho_s d_p \sqrt{\Theta_s}$.
Solids granular pressure is defined as:

$$P_s = \rho_s \varepsilon_s \left(1+4\eta g_0 \varepsilon_s\right)\Theta_s \qquad [7]$$

The collisional dissipation of granular energy is defined as:

$$J_s = \frac{12\left(1-e^2\right)}{d_p\sqrt{\pi}}\varepsilon_s^2 g_0\ \Theta_s^{1.5} \qquad [8]$$

The only constitutive relation needed to close the solids governing equations, which was not derived from kinetic theory, is the gas/solids friction coefficient (β). We use in this study the well-known Wen and Yu correlation (as defined by Gidaspow, 1994 or Agrawal et al., 2001):

$$\beta = \frac{3}{4} C_D \frac{\rho_g \varepsilon_g \varepsilon_s \left| \mathbf{u}_g - \mathbf{u}_s \right|}{d_p} \varepsilon_g^{-2.65} \qquad [9]$$

Where $C_D = \begin{cases} 24/\mathrm{Re}\left(1 + 0.15\mathrm{Re}^{0.687}\right) & \mathrm{Re} < 1000 \\ 0.44 & \mathrm{Re} \geq 1000 \end{cases}$ and $\mathrm{Re} = \frac{\rho_g \varepsilon_g \left| \mathbf{u}_g - \mathbf{u}_s \right| d_p}{\mu_g}$.

Time-averaged constitutive relations

All constitutive relations presented in the previous section are non-linear, and thus, the resulting time-averaged expressions need to be approximated using Taylor series. These series expansions will yield polynomials of order n in fluctuating variables and the coefficients will be analytical expressions of derivatives divided by a factorial of n. Whether such series converge or not and how many terms (the first term in the series corresponds to the 0th order polynomial) are needed to express the non-linear constitutive relations are the subjects of this section.

The first example of a constitutive relation derived from KTGF is the collisional dissipation term. The time averaging of this term has been analyzed by Hrenya and Sinclair (1997) who gave this expression:

$$\bar{J}_s = \frac{12}{\sqrt{\pi} d_p} \overline{\varepsilon_s^2 g_0 \, \Theta_s^{1.5}} = \frac{12}{\sqrt{\pi} d_p} \overline{f_1(\varepsilon_s) f_2(\Theta_s)} \approx \frac{12}{\sqrt{\pi} d_p} \left[f_1(\bar{\varepsilon}_s) f_2(\bar{\Theta}_s) + f_1^{\varepsilon} f_2^{\Theta} \, \overline{\varepsilon_s' \Theta_s'} \right] \qquad [10]$$

Where $f_1^{\varepsilon} = \left(\frac{\partial f_1}{\partial \varepsilon_s} \right)_{\bar{\varepsilon}_s}$ and $f_2^{\Theta} = \left(\frac{\partial f_2}{\partial \Theta_s} \right)_{\bar{\Theta}_s}$.

Recognizing the separation of variables in the collisional dissipation term, equation (10) is just a Taylor series expansion that only includes the 0th and 1st order polynomial. Stopping the series expansion at the 2nd term can only be motivated by small fluctuations in the flow variables. However, we have seen in Figure 1 that large oscillations are computed by the transient model, and thus, such a limited expansion may not be valid.

To show that such Taylor expansion may not even converge, let's take a simple example of the function $\bar{f}_2(\Theta_s) = \overline{\Theta_s^{1.5}}$ and expand it about the mean:

$$\bar{f}_2(\Theta_s) = \underbrace{\underbrace{\underbrace{f_2(\bar{\Theta}_s)}_{term\,1} + \underbrace{f_2^{\Theta} \overline{\Theta_s'}}_{=\,zero}}_{term\,2} + \frac{1}{2!} f_2^{2\Theta} \overline{\Theta_s'^2}}_{term\,3} + \frac{1}{3!} f_2^{3\Theta} \overline{\Theta_s'^3} + \underbrace{\frac{1}{4!} f_2^{4\Theta} \overline{\Theta_s'^4} + \ldots}_{term\,4} \qquad [11]$$

Because of the large amplitude of oscillations in the granular temperature, the Taylor series expansion of function f_2 diverges in regions near walls for the high order terms. After recognizing that terms in the Taylor series expansion alternatively change sign, the Euler transformation was used (Press et al., 2006) when the high order terms start diverging (this is indicated by an increase in the absolute value of the nth term in comparison with the n-1 term) . Figure 2-b shows that a good convergence is achieved with the Euler transformation.

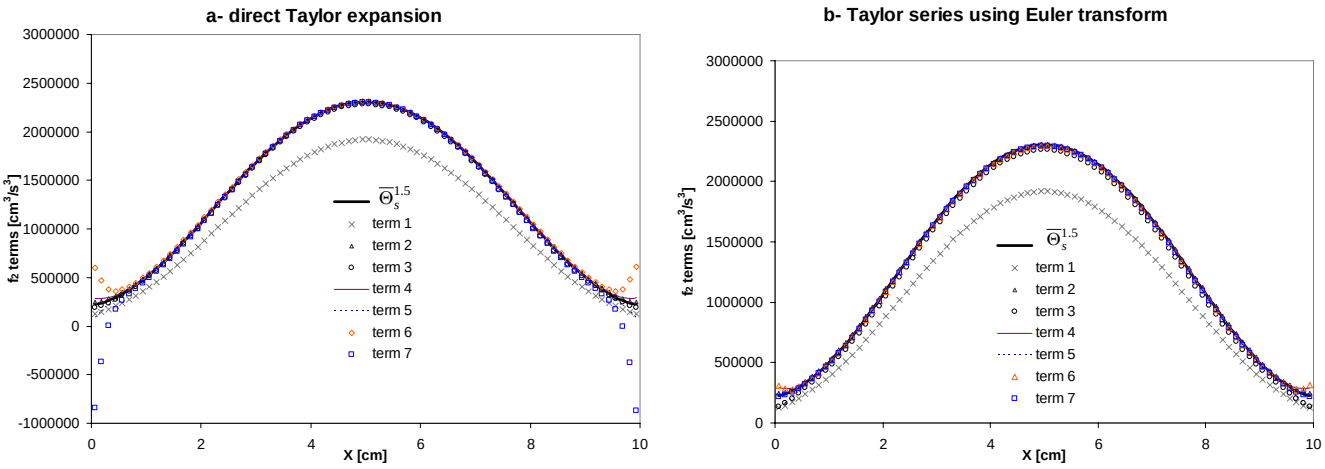

Figure 2 The diverging Taylor series expansion is made to converge using the Euler transformation.

Figure 2-a shows that the Taylor series expansion diverges when using high order terms, but does not show the need for taking higher order terms since using up to term 2 seems to fit the function f_2 reasonably well. So we turn our attention to our original problem of expanding the function $f_1 f_2$ about mean values:

$$\overline{f_1(\varepsilon_s) f_2(\Theta_s)} = \underbrace{\underbrace{f_1(\bar{\varepsilon}_s) f_2(\bar{\Theta}_s)}_{term1} + f_1^{\varepsilon} f_2^{\Theta} \overline{\varepsilon'_s \Theta'}_s}_{term\ 2} + \underbrace{\frac{1}{2!}\left(f_1 f_2^{2\Theta} \overline{\Theta'^2_s} + f_1^{2\varepsilon} f_2 \overline{\varepsilon'^2_s} + f_1^{\varepsilon} f_2^{2\Theta} \overline{\varepsilon'_s \Theta'^2_s} + f_1^{2\varepsilon} f_2^{\Theta} \overline{\varepsilon'^2_s \Theta'_s} + f_1^{2\varepsilon} f_2^{2\Theta} \overline{\varepsilon'^2_s \Theta'^2_s} \right) + \ldots}_{term\ 3} \quad [12]$$

Where, for e.g., $f_2^{2\Theta} = \left(\frac{\partial^2 f_2}{\partial \Theta_s^{\,2}} \right)_{\bar{\Theta}_s}$. All derivatives were analytically derived using Maxima 5.9.2 software (http://maxima.sourceforge.net), which was also used to generate Fortran 90 code to compute derivatives in MFIX.

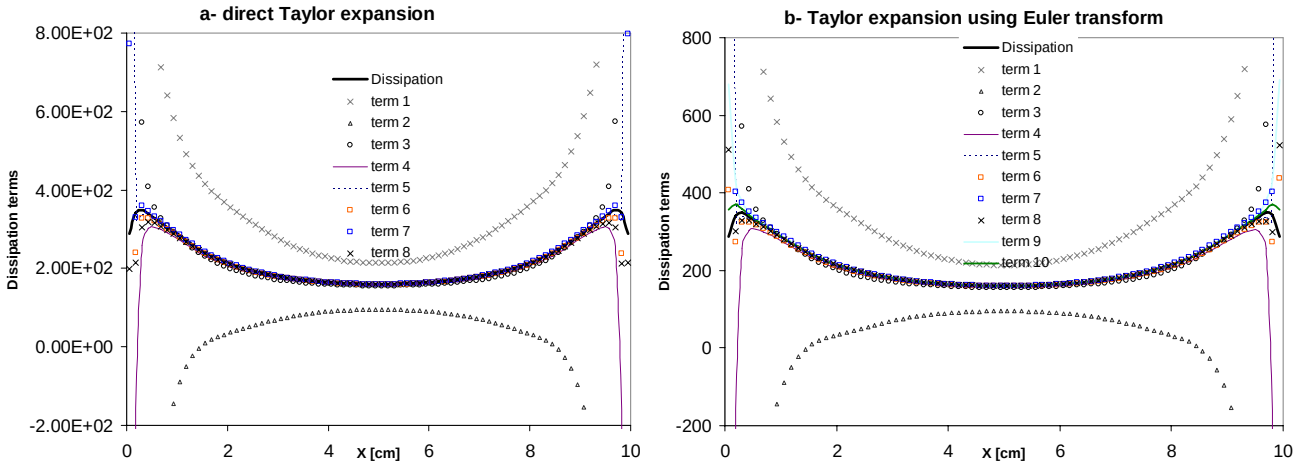

Figure 3 Convergence behavior of the Taylor series expansion of the dissipation terms with and without Euler transformation.

In Figure 3, Euler transformation is implemented for the 5th and higher terms where we observed an increase, or divergence, in the magnitude of the terms. It is noteworthy mentioning that term 2 or the expansion used in equation (10) is not a satisfactory representation in both shape and magnitude (near-wall large negative values are computed) of the time averaged collisional dissipation. We had to continue the expansion to the 10th term using Euler transformation in order to obtain a reasonably converged series expansion. The previous study of Hrenya and Sinclair assumed the same form for the dissipation as equation (10) due to the assumption of small fluctuations. However, this study proves that such an assumption is not reasonable. Also Figure 3 shows that most of the disagreement in the Taylor series expansion occurs near the walls because the largest fluctuations in volume fractions are computed near the walls where dense clusters form (see figure 1-a).

A similar behavior is observed for the Taylor series expansion of solids viscosity where the Euler transform is required to obtain a converged series. Here again, Euler's technique makes this diverging series to converge because of the alternating sign of the series terms. It is clear from Figure 4 that the "laminar" viscosity $\mu_s\left(\overline{\varepsilon}_s, \overline{\Theta}_s\right)$ or the first term in Taylor series expansion will overpredict the time-averaged viscosity and so that higher order terms in the Taylor series expansion must be considered.

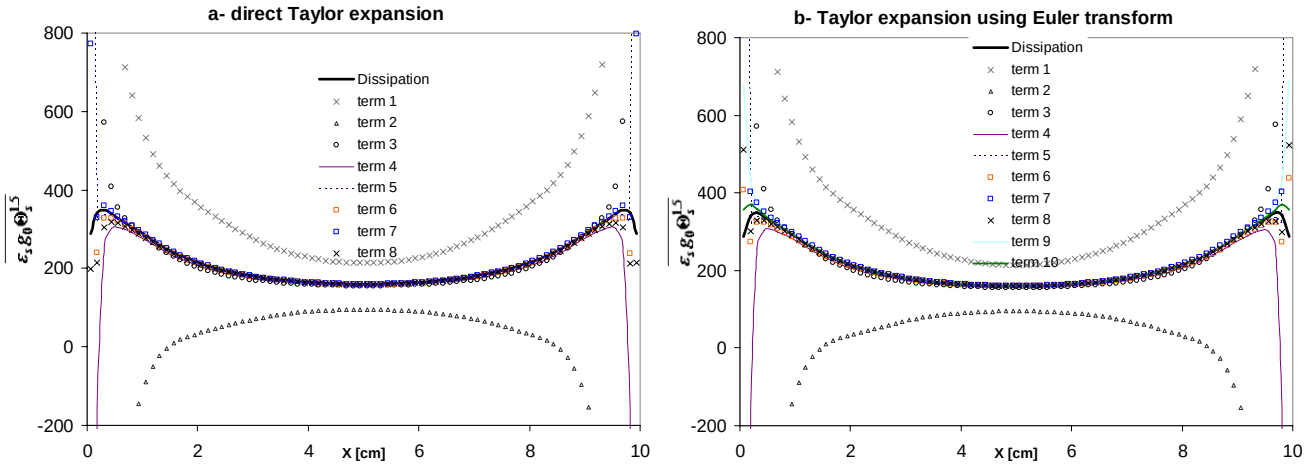

Figure 4 Convergence behavior of the Taylor series expansion of the solids viscosity terms with and without Euler transformation.

The effect of solids viscosity in the vertical momentum equation is introduced as $\overline{\mu_s \frac{\partial v_s}{\partial x}}$, so that it's not enough to obtain just the values of $\overline{\mu}_s$. We develop the time-averaged shear stress in the following manner:

$$\overline{\mu_s \frac{\partial v_s}{\partial x}} = \overline{\mu_s \frac{\partial\left(\overline{v}_s + v_s'\right)}{\partial x}} \qquad [13]$$

In equation (13), we make use of the Taylor series expansion already developed for $\overline{\mu}_s$, and each of these terms will be multiplied by the instantaneous and averaged velocity gradient, which doubles the number of terms (or correlations) in the original series for $\overline{\mu}_s$.

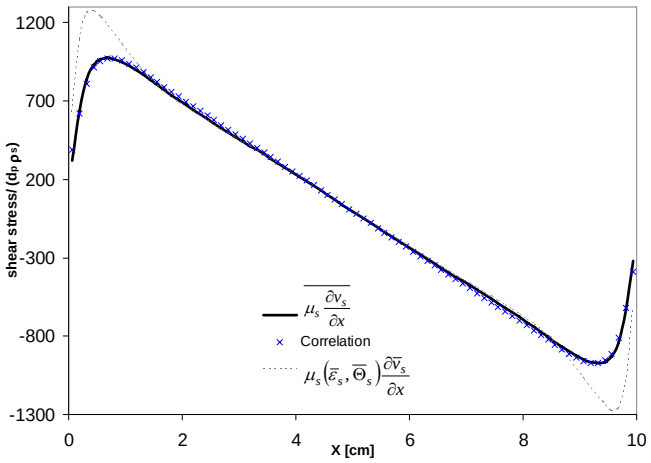

Figure 5 Comparison between time-averaged shear stress, Taylor series expansion (correlation) and "laminar" shear stress.

Figure 5 shows the "laminar" or 0th order polynomial in Taylor series expansion and the "turbulent" or time-averaged shear stress results are similar in the middle of the channel except near the walls where relatively large differences occur. It's clear that correlations of fluctuating volume fraction, granular temperature and gradient of solids velocity cannot be neglected. It is remarkable that the effect of the non-linearity of the shear stress term is noticeable before even mentioning the contribution of Reynolds stress terms that rise from the time-averaging of the convective terms. However, we'll address the importance of the shear stress next in this section when we show the computed results of Reynolds stresses.

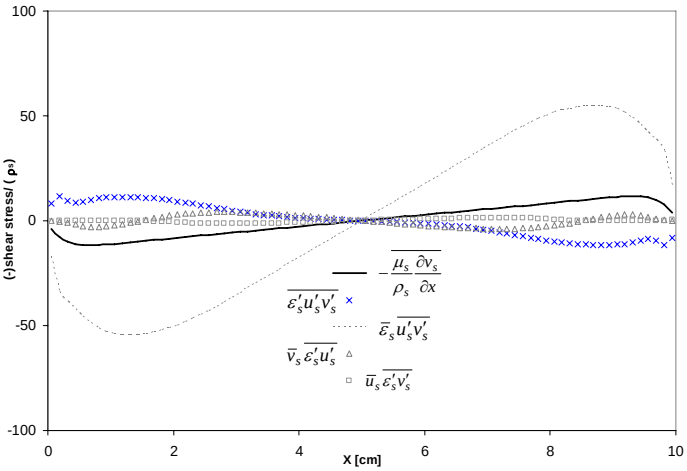

Figure 6 Comparison between different Reynolds-like stresses and time-averaged shear stress

It is clear from Figure 6 that the major contribution to the shear stresses will be from the traditional Reynolds stress $\bar{\varepsilon}_s \overline{u_s' v_s'}$. The contribution of the triple correlation $\overline{\varepsilon_s' u_s' v_s'}$ has opposite sign (will contribute a negative turbulent viscosity) and has similar magnitude as compared to the time-averaged shear stress. However, the sum of shear stresses will obviously yield a positive turbulent viscosity because

$\bar{\varepsilon}_s \overline{u_s' v_s'}$ has a larger magnitude. The smallest contribution to the turbulent stresses is due to $\bar{u}_s \overline{\varepsilon_s' v_s'}$ because the average of the radial velocity is negligible.

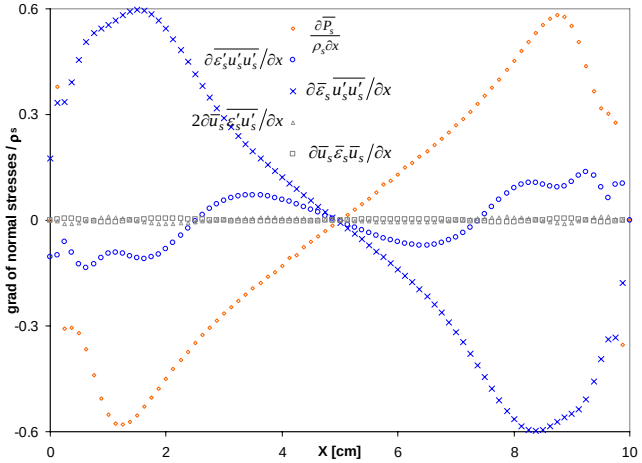

Figure 7 Comparison between gradients of different normal Reynolds stresses and time-averaged solids pressure

Figure 7 shows horizontal profiles of the gradients of time-averaged solids pressure and normal Reynolds stresses. Again, all terms involving $\bar{u}_s$ are negligible and the most important terms are due to gradients of solids pressure and normal stress $\partial \bar{\varepsilon}_s \overline{u_s' u_s'}/\partial x$. This is quite different from the analysis of the shear stresses where the time-averaged shear stress was not as significant as the Reynolds shear stress. Because of the importance of solids pressure, as seen in Figure 7, it is necessary to ensure that the Taylor series expansion of this expression is properly conducted. We also recognize that the solids pressure is not a linear function of solids volume fraction, but is a linear function of granular temperature. However, the time-averaged solids pressure must be correlated in a similar manner as in equation (12). The results of the Taylor series expansion are presented in Figure 8. Note that in this case we did not need to use the Euler transformation since this series converged because of the linear dependence of solids pressure on the granular temperature. It is clear from figure 8 that using the steady-state values (1st term) or even the second term in Taylor series expansion (2nd term) will hinder the ability of a reduce model to accurately represent the time-averaged solution (note that near-wall data for some terms were not plotted because they lay outside the scale, which was chosen to better visualize convergence of higher order terms).
We have shown at the beginning of this section the importance of correctly expanding the dissipation of granular energy (see figure 3). Let's now shift our attention to the production due to shear of granular energy: $\overline{\mu_s \frac{\partial v_s}{\partial x} \frac{\partial v_s}{\partial x}}$.
Figure 9 shows that the correlation obtained by using Taylor series expansion of the production term (up to 7th order following same procedure as in equations 12 and 13) fits reasonably well the time-averaged production of granular energy. The laminar expression, or 1st term in the Taylor expansion, fails to capture the significant production of granular energy at the center of the channel because the time-averaged velocity gradient is zero at that location. Figure 9 shows that properly correlating the term:
$\overline{\frac{\partial v_s}{\partial x} \frac{\partial v_s}{\partial x}} = \frac{\partial \bar{v}_s}{\partial x} \frac{\partial \bar{v}_s}{\partial x} + \overline{\frac{\partial v_s'}{\partial x} \frac{\partial v_s'}{\partial x}}$ captures the high energy production at the center of the channel even

though the overshoot near the walls is exaggerated due to the approximation of laminar solids viscosity as was seen previously during the study of the shear stress (see Figure 5).

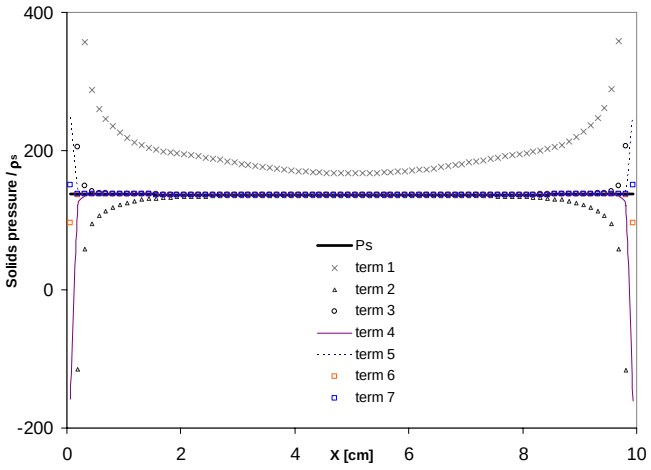

Figure 8 Simple (Euler transformation was not used) Taylor series expansion of time-averaged solids pressure

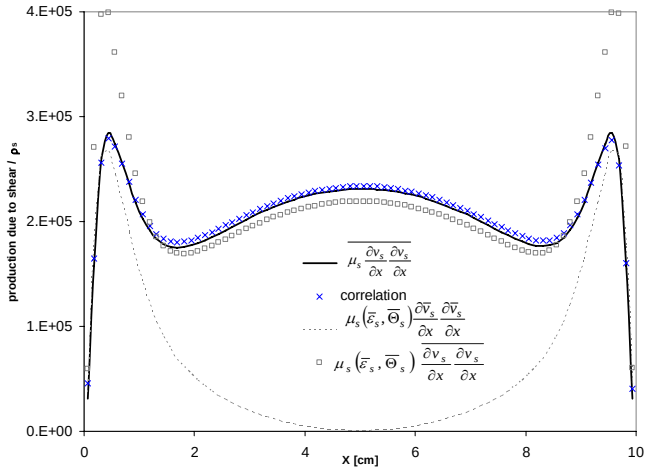

Figure 9 Comparison between time-averaged and "laminar" (or first term in Taylor series expansion) production of granular energy

Other terms arising from the time-averaging of the granular temperature equation (see equation 4) such as granular conductivity and convection terms will be ignored and we will demonstrate later that properly correlating the production and dissipation of granular energy is sufficient to obtain accurate profile of granular temperature.

Let's turn our attention to terms that do not arise from kinetic theory of granular flows such as $\bar{I}_{gsy}$ and $\overline{\varepsilon_s \frac{\partial P_g}{\partial y}}$. First, the solids volume fraction and axial pressure gradient are not correlated as shown in Figure 10, and thus the following equality is satisfied:

$$\overline{\varepsilon_s \frac{\partial P_g}{\partial y}} = \bar{\varepsilon}_s \frac{\partial \bar{P}_g}{\partial y} + \overline{\varepsilon_s' \frac{\partial P_g'}{\partial y}} \cong \bar{\varepsilon}_s \frac{\partial \bar{P}_g}{\partial y} \quad [14]$$

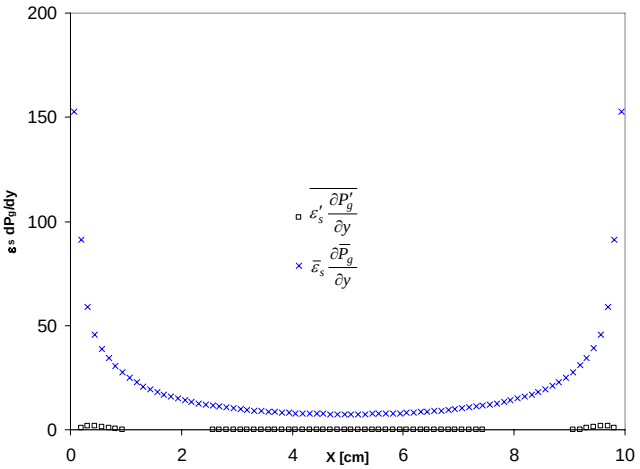

Figure 10 Verification that the solids volume fraction and gas pressure gradient are not correlated

Now, let's focus on the gas/solids momentum exchange I_{gsy}, which is arguably one of the most important terms in the momentum equations that describe fluidization processes. Let's first assume that the momentum exchange term is less important in the horizontal direction, so that we can focus on deriving a series expansion of the $\bar{I}_{gsy}$ term in the vertical direction only, which yields: $-\bar{I}_{gsy} = \overline{\beta\left(v_g - v_s\right)}$. If we assume that the magnitude of the relative velocity is equal to the absolute value of the vertical component of the relative velocity, then we can show that equation (9) reduces to:

$$-\bar{I}_{gsy} = 18\mu_g \overline{\frac{\left(1-\varepsilon_g\right)}{\left(\varepsilon_g^{2.65} d_p^2\right)} V_r \left(0.15\left(\varepsilon_g \rho_g |V_r| d_p / \mu_g\right)^{0.687} + 1\right)} \quad [15]$$

Here we note that $V_r = v_g - v_s$, which shows less that 0.1% error in computing equation (15) as compared with using the magnitude of relative velocity instead. Also there is no loss of accuracy in assuming that the Re number is always less than 1000 in this study so that C_D is formulated using only one expression (see equation 9). Since in equation (15), one would recognize that it is not possible to separate the volume fraction and relative velocity as was done in equation (12), so that equation 15 needs to be expanded in a Taylor series of two variables (see for e.g. Greenberg, 1998, page 638). In general, we can express using a loose mathematical notation (for more details see http://mathworld.wolfram.com/TaylorSeries.html) the Taylor series of two variables as:

$$-\bar{I}_{gsy} = f\left(\varepsilon_g, V_r\right) = \sum_{j=1}^{\infty} \left\{ \frac{1}{j!} \left(\varepsilon_g' \frac{\partial}{\partial \varepsilon_g} + V_r' \frac{\partial}{\partial V_r} \right)^j f\left(\bar{\varepsilon}_g, \bar{V}_r\right) \right\} \quad [16]$$

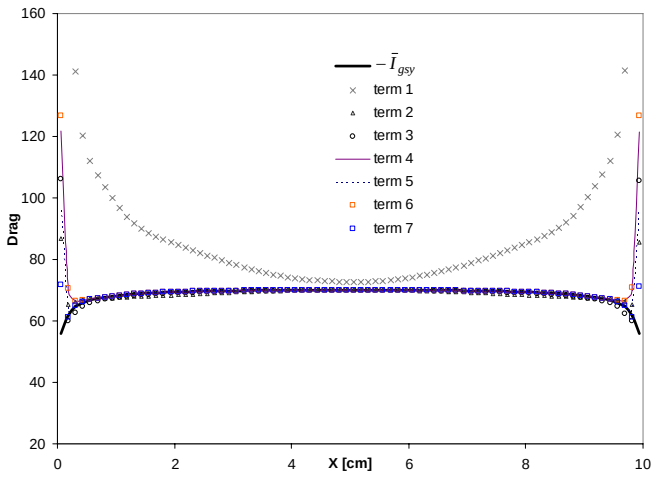

Figure 11 Convergence check on the Taylor series expansion of the gas/solids momentum exchange

Figure 11 shows that a Taylor series expansion of the function of two variables eventually converges without a need of using Euler transformation. Again, the laminar, or first term, fails to predict the qualitative behavior of the time-averaged function and higher order terms have difficulty capturing the large oscillations and coupling of void fraction and slip velocity near the walls. Another difficulty is the large amount of computer code generated by the derivatives used in the Taylor series expansion: the gas/solids drag (up to the 7^{th} term), for e.g., uses about 1000 line of Fortran code (derivatives for viscosity formulation use a bit more than that). Furthermore, the large amount of correlations generated from time-averaging governing equations, such as correlations between volume fraction and granular temperature, makes this approach difficult to apply in industrially-significant processes. Definitely, more research is needed in multiphase flow turbulence modeling in order to produce ROM with similar accuracy as in single-phase flow (e.g. k-epsilon model).

So far we have not conducted the time-averaging of gas governing equations because of the observation that the gas phase reacts to the motion of solids, i.e. transient motion of the gas/solids flow in this study does not occur because of turbulence in the gas phase but is due to clustering of particles as was established previously by Benyahia et al. (2007). Figure 12 shows that the most important contribution to the stresses is from the traditional Reynolds shear stress $\bar{\varepsilon}_g \overline{u'_g v'_g}$ as all other terms from the averaging of gas convection are negligible. A remarkable difference in the analysis of gas and solids stresses is that the gas laminar stress $\overline{\frac{\mu_g}{\rho_g}\frac{\partial v_g}{\partial x}}$ is of different sign than the Reynolds stress $-\bar{\varepsilon}_g \overline{u'_g v'_g}$, which is just the opposite of our previous findings for the solids phase (see Figure 6). Furthermore, the sum of all shear stresses in the gas phase show that a negative turbulent viscosity is computed in most of the 1-D flow domain, which is counterintuitive based on our knowledge of single-phase turbulence models. However, it is easy to demonstrate that the sum of both gas and solids turbulent (dynamic) viscosity will be positive due to the fact that solids to gas density ratio is about three orders of magnitude.

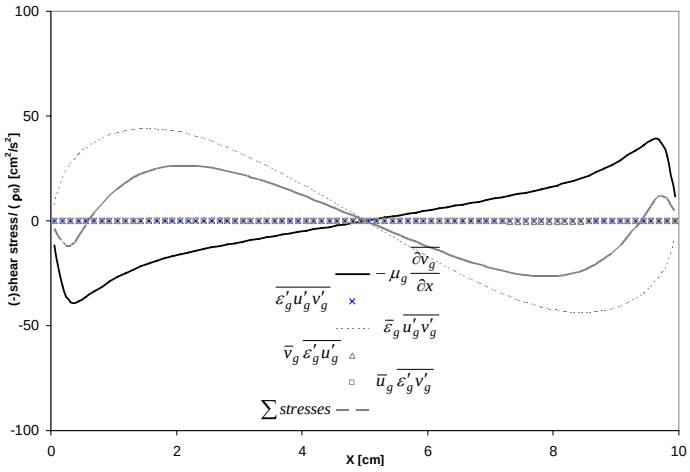

Figure 12 Laminar and Reynolds shear stresses in the gas-phase showing negative values of "turbulent" gas viscosity in most regions of 1-D riser except near walls.

A physical explanation for the negative gas turbulent viscosity reported in Figure 12 can be obtained by looking at the instantaneous gas and solids horizontal and vertical velocity profiles plotted in Figure 13. It shows that although the instantaneous vertical velocity of solids and gas have similar profiles, the horizontal velocity profiles have same magnitude but opposite sign. Thus, vertically the solids follow the gas closely because of drag, but horizontally the solids move from one side of the channel to the other due to cluster formation, as explained by Benyahia et al, 2007, and the gas moves to regions vacated by the solids because of volume fraction conservation ($\varepsilon_g = 1 - \varepsilon_s$). For this reason, we plotted in Figure 13 the horizontal volumetric flux ($u\varepsilon$) to show that instantaneous solids and gas volumetric flux profiles are the same in magnitude with opposite sign. So in relatively dense systems such as the one studied here, we view gas turbulence just as a reaction to solids motion which can be described in sufficient accuracy using the granular kinetic theory as demonstrated by Benyahia et al. (2007) who found that gas/solids flow patterns were not affected by the gas turbulent stress derived from modified k-epsilon models.

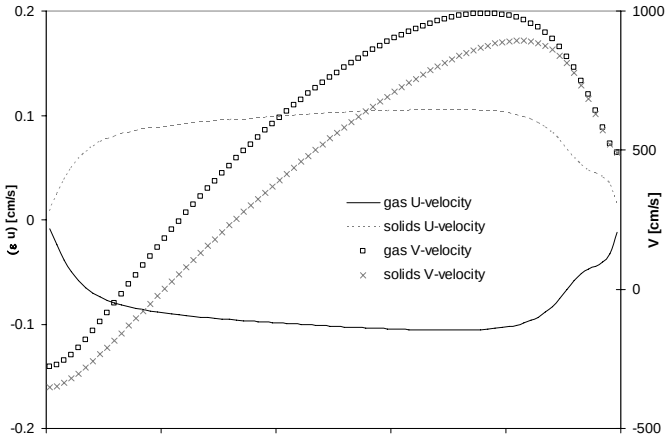

Figure 13 Instantaneous gas and solids horizontal flux (εu) and vertical (V) velocities.

Steady-state results

Steady-state results are obtained by adding to the governing equations the Taylor series expansion of all non-linear and Reynolds stress terms identified in the previous section of this study. We still used the transient terms in the governing equations and started the simulation from a uniform (flat horizontal profiles were used) initial state where solids volume fraction was set to 0.03, solids and gas vertical velocities were set to 5.2 and 5.5 respectively, granular temperature was set to 0.1 m^2/s^2 and finally zero horizontal gas and solids velocities.

Starting from a uniform initial state, a major difficulty for the algorithm in MFIX to converge using the steady-state model was the fact that the Taylor series expansion of positively bounded functions, such as solids pressure, production and dissipation of granular energy etc., can become negative. In fact, the only guarantee for the Taylor series to fit, for example, the granular energy dissipation is by using the steady-state values of solids volume fraction and granular temperature. Different values of these flow variables lead to unphysical values of the granular dissipation and other positively bounded constitutive relations, which prevented the flow algorithm from converging. We also tried a "realizability" criterion that assumes $\overline{f_1(\varepsilon_s) f_2(\Theta_s)} = f_1(\overline{\varepsilon}_s) f_2(\overline{\Theta}_s)$ in case equation 12 yields negative values of $\overline{f_1(\varepsilon_s) f_2(\Theta_s)}$, and this criterion was applied to all the Taylor series expansion of non-linear terms used in this study. Unfortunately, the algorithm did not converge unless the granular energy dissipation and production use the time-averaged values of solids volume fraction and granular temperature to compute the derivatives in equation 12. Still, the algorithm converged only for initial solutions that are close to the steady solution, and the final solution deviated from the time-averaged solution because the realizability criterion was constantly applied in the algorithm at computational cells next to walls.

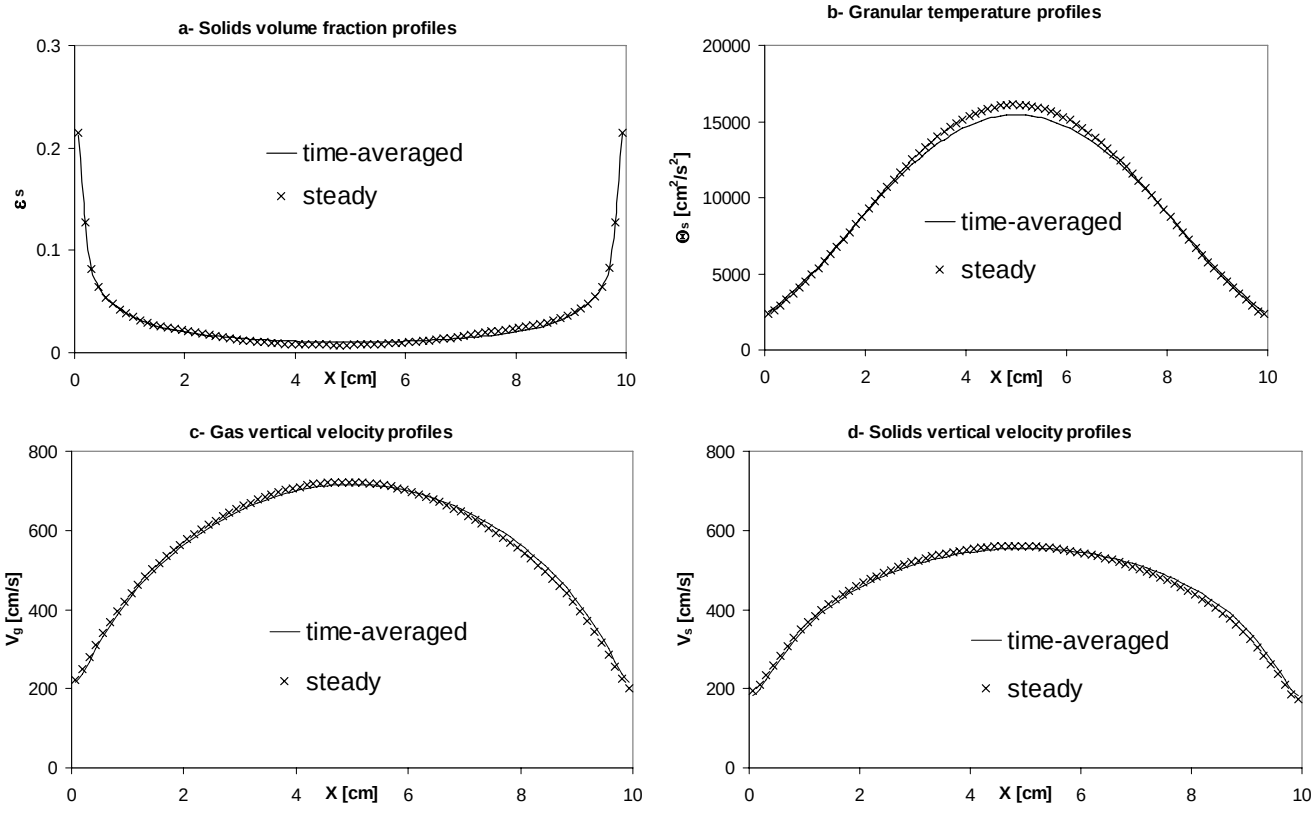

Figure 12 Comparison of time-averaged and steady-state results using all correlations arising from time-averaging non-linear terms in solids momentum and granular energy equations.

Using the fully fitted non-linear terms in the governing equations, the transient simulation converged to a steady-state after few seconds of simulation. The results reported here were obtained after 10 sec of simulation. We compare the steady results with time-averaged results obtained using a transient model that doesn't use any correlations.
Figure 12 shows good comparison of time-averaged transient results and steady-state results obtained by using all correlations presented in this study. It took only few minutes of CPU time to compute the steady results shown in Figure 12. In contrast, it took about 6 hours of CPU time to compute 70 sec of simulation used to obtain the time-averaged results presented in Figure 12. This figure also shows that the granular temperature was slightly over-predicted at the center of the channel mainly due to a higher production of granular energy as seen in Figure 9, which also caused the solids volume fraction to be slightly under-predicted at the center of the channel. We should mention that some non-linear terms were not accounted for (without much loss of accuracy) in the steady model, namely all the correlations from the gas momentum equation, conductivity and convection terms in the granular energy equation, as well as gas/solids drag term in the solids horizontal momentum equation.

Conclusions

We demonstrated in this study that large oscillations are computed in gas/solids flows that required a large number of correlations when non-linear constitutive relations are expanded using Taylor series. Oscillations in the gas phase were found to be only a reaction to the motion of the solids phase in this moderately dense system. This study demonstrates that it is possible to obtained steady-state results that match the time-averaged computational results of a transient model. However, such a model seems impractical because of the large number of correlations that need to be modeled and also due to convergence difficulties.

Nomenclature

d_p: particle diameter.

e: particle-particle restitution coefficient.

g_i : acceleration of gravity in the i direction.

g_0 : radial distribution function at contact.

I_{gs}: gas/solids momentum exchange.

J_s: granular energy dissipation due to inelastic collisions.

P_m: pressure of phase m.

S_{mij}: mean strain-rate tensor.

u_m, v_m: instantaneous horizontal and vertical velocity components of phase m.

Greek letters:

β: gas/solids friction coefficient.

ε_m: volume fraction of phase m.

η: constant depending on particle restitution coefficient equal to $(1+e)/2$.

κ: solids phase dilute granular conductivity.

κ_s: conductivity of solids granular energy.

μ : solids phase dilute granular viscosity.

μ_b : bulk viscosity of the solids phase.

μ_g : dynamic viscosity for gas phase.

Θ_s : granular temperature.

ρ_m : density of phase m.

τ_{mij} : stress tensor of phase m.

Indices:

g: gas phase.
i, j: indices used to represent spatial direction.
m: phase m: g for gas and s for solids phases.
max: maximum packing.
s, p: solids, particulate phase.

References

Agrawal K, Loezos PN, Syamlal M, Sundaresan S. J. Fluid Mech. 2001;445:151-185.
Benyahia S, Syamlal M, O'Brien TJ. AIChE J. 2007; 53:10, DOI 10.1002/aic.11276.
Dasgupta S, Jackson R, Sundaresan S. AIChE J. 1994, 40:2;215-228.
Elghobashi SE, Abou-Arab TW. Phys. Fluids 1983;26:4;931-938.
Gidaspow D. Multiphase flow and fluidization: continuum and kinetic theory description. San Diego: Academic Press, 1994.
Greenberg MD, Advanced engineering mathematics, 1998. Prentice Hall NJ.
Hrenya CM, Sinclair JL. AIChE J. 1997;42:853-869.
Lun CKK, Savage SB, Jeffrey DJ, Chepurniy N. J Fluid Mech. 1984;140:223-256.
Press WH, Teukolsky SA, Vetterling WT, Flannery BP, Numerical recipes in Fortran 77, 2006. Cambridge Univ. Press, NY.